Research Article

Journal of PeptideScience

Received: 9 June 2010 Revised: 4 August 2010 Accepted: 6 August 2010 Published online in Wiley Online Library: 27 September 2010

(wileyonlinelibrary.com) DOI 10.1002/psc.1295

Conformational space search of Neuromedin C using replica exchange molecular dynamics and molecular dynamics

Parul Sharma,[a] Parvesh Singh,[a]* Krishna Bisetty,[a] Alex Rodriguez[b] and Juan J. Perez[b]

The present study involves the utilization of replica exchange molecular dynamics (REMD) methodology to explore the conformational space of Neuromedin C (NMC) using implicit ($REMD^{implicit}$) and explicit ($REMD^{explicit}$) water models. Comparison of the structures obtained from these simulations indicate that $REMD^{explicit}$ trajectory display a greater tendency to induce β-turns and bent structures as compared to those obtained from the $REMD^{implicit}$ simulation. Moreover, two additional MD trajectories performed using Langevin (MD^{Lang}) and Berendsen (MD^{Berend}) algorithms under generalized born (GB) solvent conditions were also suitably competent to sample similar kinds of conformations, although the extent of beta turns was low compared to those observed in $REMD^{explicit}$ simulation. Finally, the comparison of results obtained from all the trajectories and those derived from the NMR studies of Ni(II) complex of NMC indicates that the REMD under explicit conditions is more efficient in sampling the conformations, and show good agreement with the experimental results. Copyright © 2010 European Peptide Society and John Wiley & Sons, Ltd.

Keywords: NMC; REMD; MD; hydrogen bond; β-turn; NMR; generalized born (GB); CLASICO

Introduction

Neuromedins, bombesin-like peptides, are known to be widely distributed in the mammalian gastrointestinal tract, spinal cord and brain. Neuromedin C (NMC) and Neuromedin B (NMB) are novel decapeptides that have recently been isolated from porcine spinal cord and canine intestinal mucosa and show striking sequence homology with bombesin and gastrin-releasing peptide (GRP-27) at the carboxyl-terminal region [1,2]. NMC acts as a growth factor in a wide range of tumors including carcinomas of the pancreas, stomach, breast, prostate, and colon [3]. As Bombesin and GRP are reported to bind to the GRP receptor with high affinity [4] triggering activation of protein kinase C, elevation of cyclic-AMP levels and the stimulation of tyrosine kinases [2], it is likely that NMC that shares the last ten residues of GRP could bind to this receptor.

Recently, NMR spectroscopy and MD simulations [5] in aqueous solution have been employed to determine the structure of the 27-residue GRP. Only a short helical structure was observed in the *N*-terminal region and the overall structure of the GRP peptide did not show any ordered secondary structure, similar to the observations made for other peptide hormones in aqueous solution [6]. Bombesin, on the other hand, has been reported to adopt helical conformations between residues 4 and 10 on the basis of its NMR experiments in the presence of a 50% trifluroethanol–water mixture [7,8]. Additionally, CD studies of NMC, equivalent to last 18–27 residues of GRP, in the water-lipid environment suggest that the peptides in a polar medium exist in a very flexible structure, and are, to some extent, α-helical in a nonpolar medium [9]. Moreover, 2D-NMR experiments have demonstrated that NMC adopts two well-defined turns after forming a complex with Ni(II) using its initial three *N*-terminus residues [10]. The first turn corresponds to the Ni(II) coordination ligands in a square planar conformation, and the second reveals the interaction between the fourth (Tryptophan) and the eighth residue (Histidine).

NMC, being shorter in size, is quite flexible to take on several different conformations, making assessment of its bioactive conformation quite challenging. Therefore, despite having great biological and pathological significance [3], a unique native conformation of NMC has not been to date clearly elucidated on the basis of available spectroscopic results.

While experimental knowledge is essential for the understanding of effects of counterions on the structure and dynamical properties of proteins in solutions, theoretical studies involving computer simulations complement the experimental data. In particular, MD simulations provide detailed information on the fluctuations and conformational changes of proteins and nucleic acids, and are routinely used to investigate the structure, dynamics and thermodynamics of biological molecules and their complexes [11–14]. However, the sampling efficiency of MD simulations is severely hampered by the rugged energy surface of polypeptides, with small relative free energies separating native, folded protein conformations from unfolded states. In order to allow the MD

* *Correspondence to: Parvesh Singh, Department of Chemistry, Durban University of Technology, Durban 4000, South Africa. E-mail: parveshguleria2006@yahoo.co.in*

a *Department of Chemistry, Durban University of Technology, Steve Biko Campus, P.O. Box 1334, Durban 4000, South Africa*

b *Department d' Enginyeria Quimica, UPC, ETS d'Enginyers Industrials, Av. Diagonal, 647, 08028 Barcelona, Spain*

Journal of PeptideScience

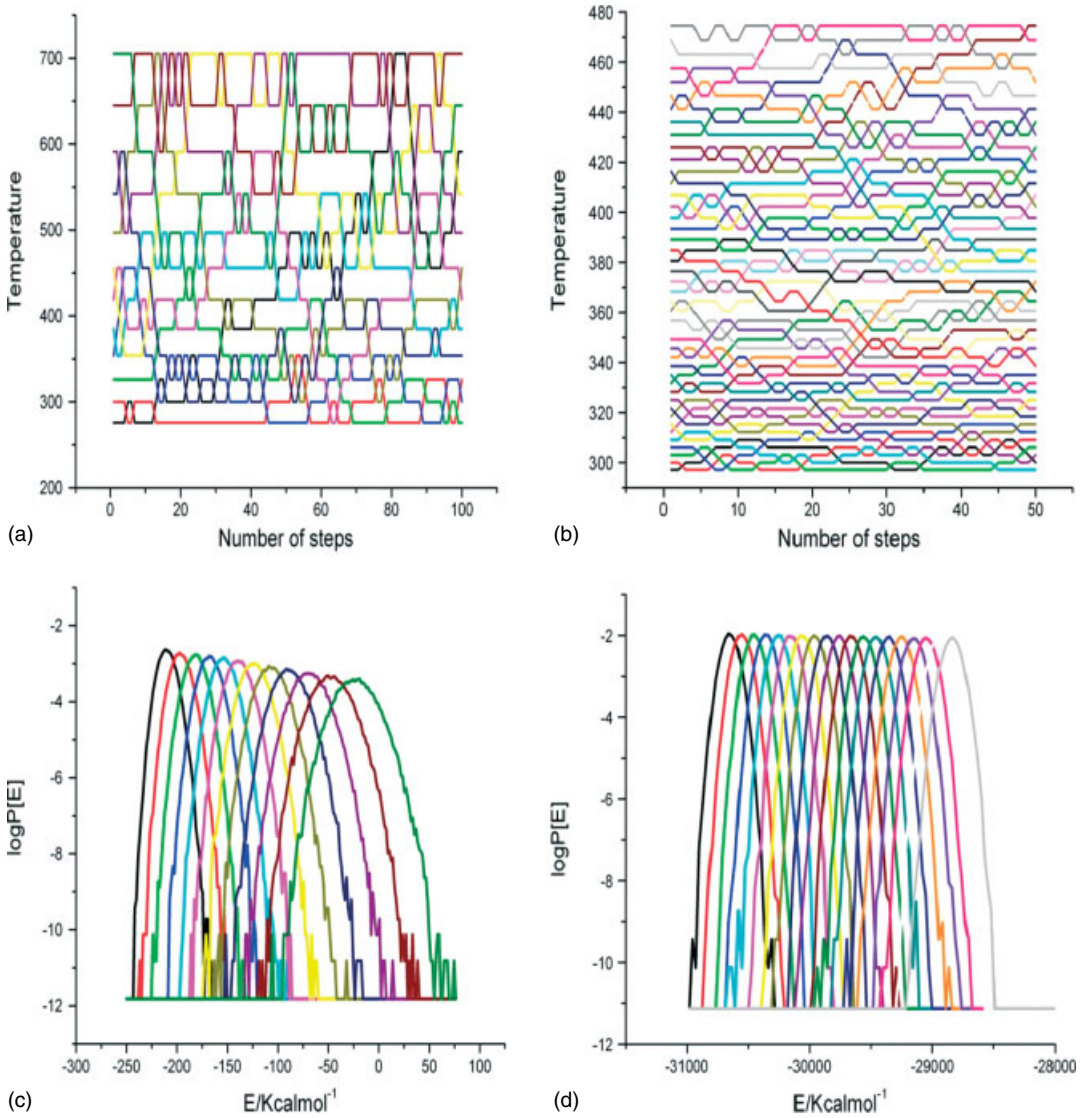

Figure 1. Time series of temperature exchange for (a) $REMD^{implicit}$ (b) $REMD^{explicit}$ and the canonical probability distributions of the total potential energy of NMC obtained from the (c) $REMD^{implicit}$ at the 12 temperatures and (d) $REMD^{explicit}$ at the 44 temperatures (only 18 shown). The distributions in (c) and (d) correspond to the temperature ranges (from left to right): 276–705 K and 297.1–474.6 K, respectively.

simulation to escape the multientrapment minima and explore a wider portion of the conformational space, enhanced sampling techniques have been developed. One of the most popular ones, replica exchange molecular dynamics (REMD), is a multicanonical sampling procedure based on running multiple parallel MD simulations or replicas of a system at increasing temperatures *T*1, *T*2, etc, allowing exchange of configurations between neighboring replicas according to a certain probability of swapping [15–17]. Thus, conformations are simulated at all temperatures and escape local minima with the kinetic energy provided at higher temperatures, while Boltzmann distributions are generated at all temperatures.

Recently, it has been demonstrated that MD simulations employing the implicit continuous model of the generalized born (GB) approximation in combination with AMBERff96 show faster and better efficiency in sampling the conformational space [18]. However, the disadvantage associated with this kind of simulations is their inability to sample those conformations which are stabilized through inter-molecular interactions with the solvent molecules, consequently enhancing more compact and bent structures. The present studies involve the conformational space search of NMC both under implicit and explicit water conditions using REMD as a sampling method. The selection of water environment for the current studies has been made on the basis of the expected binding of NMC to the cell, via a protein receptor than directly with the lipid bilayers, as reported in the literature [10,19]. Two additional MD simulations using Langevin and Berendsen algorithms were also performed using Onufriev, Bashford and Case (OBC) implicit water model [20]. Finally, NMR results were employed to validate the present computational protocols.

Computational Details

Replica Exchange Molecular Dynamics

An extended structure of NMC was generated using the leap module of AMBER 8.0 [21,22]. The *N*-terminal of the peptide was protonated, while the *C*-terminal was amidated. For implicit

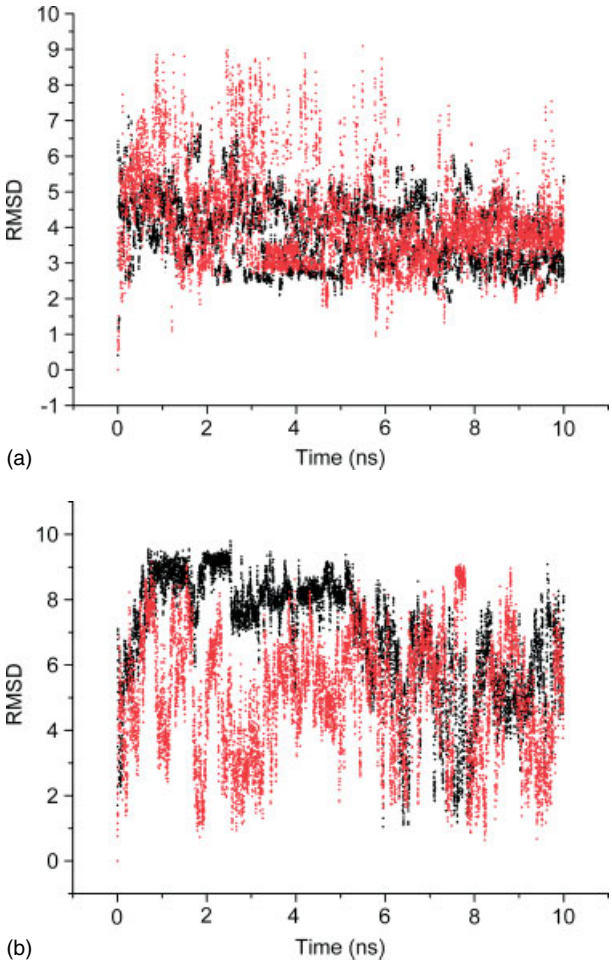

Figure 2. Root mean square deviations (backbone–backbone) of NMC from the starting structure in case of (a) REMD^{implicit} in red and REMD^{explicit} in black, (b) MD^{Lang} in red and MD^{Berend} in black. Figure 2a and b shows 1-ns segment of REMD and MD simulations respectively.

REMD, the extended structure of the peptide was energetically minimized with a convergence criterion of 0.005 kcal mol^{-1} Å^{-1}. REMD was performed on the minimized structure of NMC using OBC implementations based on the GB approximation [20]. The dielectric constant around the peptide (internal dielectric constant) was set to 1 and the external dielectric constant was set to 80, corresponding to water. Prior to the REMD simulations, standard MD simulations were performed for 5 ns at different temperatures (200–900 K range) with a gap of 100 K. In the present study, 12 replicas were used and the temperature of each replica was set at: 276, 300, 326, 354, 385, 419, 456, 497, 542, 591, 645 and 705 K. The time step was set to 0.2 fs, and the SHAKE method was used to constrain all hydrogen atoms. The temperature during MD simulations was regulated by the Langevin thermostat [23–25]. Each replica was simulated simultaneously and independently at different replica temperatures. The replica exchange was performed every 2 ps for 50 000 steps during the REMD simulations.

For REMD explicit simulation, the extended conformation of NMC was solvated in a $64 \times 50 \times 37$ Å^3 box of TIP3P [26] water box. The whole system contained 8894 atoms (2904 water molecules and 153 atoms for NMC) including 14 Na^+ and 15 Cl^- ions used to neutralize the system. In order to mimic the physiological conditions, a 0.2-M salt concentration was used. The system was then subjected to minimization with initial 5000 steps of steepest descent followed by 10 000 steps of conjugate gradient at constant volume. The energy minimization of this new system was completed when a convergence criteria of 0.001 kcal mol^{-1} Å^{-1} was fulfilled. The minimized system was heated to 300 K at constant volume in 20 ps in 50 K increments. Subsequently, the system was equilibrated for next 100 ps at constant pressure using periodic boundary conditions (PBC). Eight standard MD simulations were performed thereafter at constant volume for 5 ns in the rank of temperatures 200–900 K with a gap of 100 K. Simulations were performed with PBC and the particle mesh Ewald method was used for the treatment of electrostatic interactions [27]. A cutoff was set to 12 Å with a grid spacing of approximately 1 Å. van der Waals interactions were truncated at 12 Å with a switching function from 10 to 12 Å. For REMD, 44 replicas corresponding to the temperatures 297.1, 300, 303, 306, 309.1, 312.2, 315.3, 318.5, 321.7, 325, 328.3, 331.7, 335.1, 338.6, 342.1, 345.7, 349.3, 353, 356.8, 360.6, 364.5, 368.4, 372.4, 376.5, 380.6, 384.8, 389.1, 393.4, 397.8, 402.3, 406.9, 411.6, 416.3, 421.1, 426, 431, 436.1, 441.3, 446.6, 452, 457.5, 463.1, 468.8, 474.6 K, were chosen with a condition to have an exchange probability of 20% with the mean potential energies obtained from standard MD simulations, which are adjusted to a third-degree polynomial. REMD simulation was performed with a 2-fs time step and SHAKE algorithm [28] to constrain all bonds to hydrogens. The replica exchange was performed every 2 ps for 25 000 steps during the REMD simulation. Coordinates were saved

Journal of PeptideScience

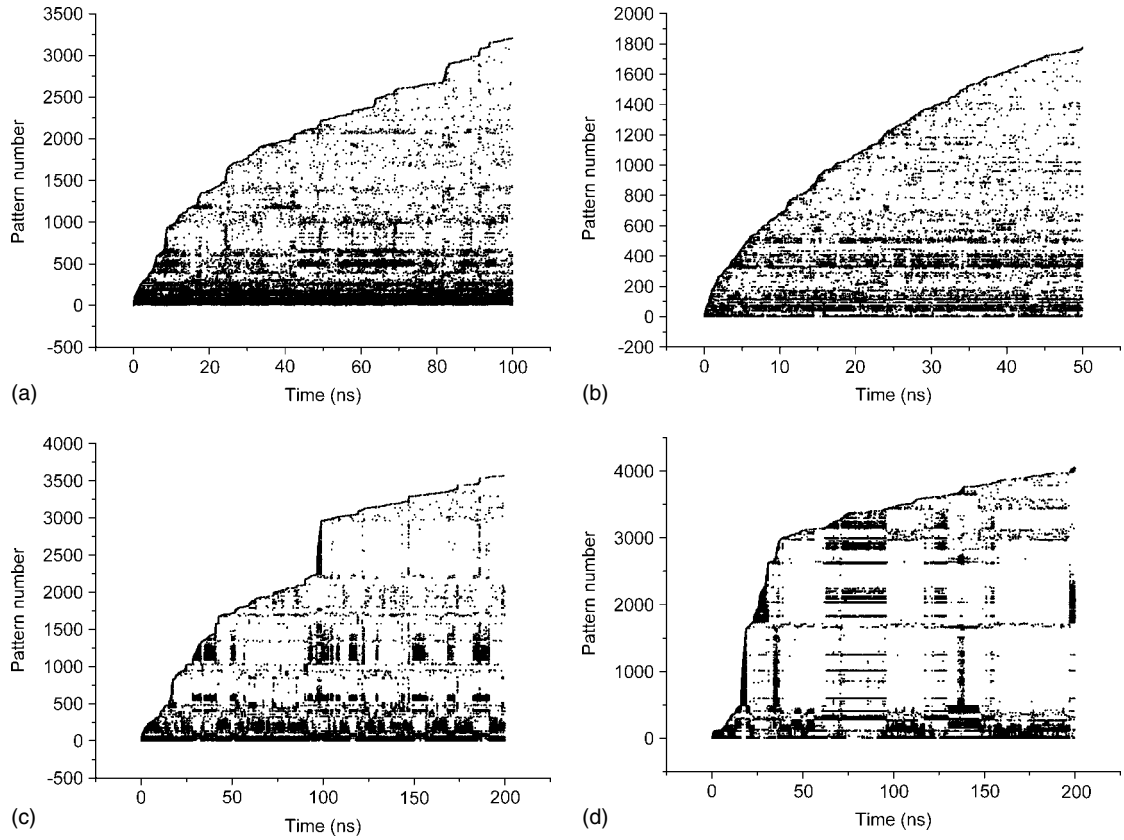

Figure 3. Evaluation of new patterns along the trajectories for the NMC in (a) REMD^{implicit}, (b) REMD^{explicit}, (c) MD^{Lang} and (d) MD^{Berend} trajectories obtained using CLASICO program. Dark areas represent trapped conformations of NMC in the configurational space.

after each picosecond. The PTRAJ module in the AMBER and the CLASICO program [29] were used to carry out the analysis of the results obtained from the simulations. The characterization of the β-turn profile for each of the trajectory was carried out using the procedure described by Corcho and co-workers [30].

Molecular Dynamics

Two MD simulations considering Langevin and Berendsen algorithms were performed at 300 K temperature using the GB approximation. The internal dielectric constant around peptide was set to 1, while the external dielectric constant of 80 corresponding to water was employed. No cut-off was considered in these investigations. In order to mimic the physiological conditions, a 0.2-M salt concentration was used. SHAKE was used on bonds involving hydrogen atoms with a time step of 2 fs.**A** similar kind of analysis, as that performed for REMD simulations described above, was employed for the MD trajectories.

Results and Discussion

Figure 1a and b shows the time series of temperature exchanges of NMC for the initial 100 steps of REMD^{implicit} and 50 steps of REMD^{explicit} trajectories respectively. Clearly, a random walk in the 'temperature space' between low and high temperature was realized in each case. Figure 1c and d, on other hand, shows the canonical probability distributions of the total potential energy along the REMD^{implicit} and REMD^{explicit} trajectories respectively, and reveals the good overlaps between all neighboring pairs of distributions suggesting their efficient performance.

Figure 2a and b shows the root mean square deviations (RMSD) of the initial 10 ns of REMD and MD trajectories respectively, monitored relative to the backbone atoms of starting structures. The RMSD values corresponding to REMD^{explicit} and MD^{Berend} simulations are shown in black, whereas those related to REMD^{implicit} and MD^{Lang} trajectories are displayed in red. Figure 2a and b clearly shows that RMSD values increase rapidly during the initial 50 ps, suggesting the initial folding steps of NMC in the trajectories. In case of REMD^{explicit}, these values oscillate between 3 and 5 Å, clearly suggesting its structural equilibrium and considerably higher fluctuations between 3 and 9 Å during the progress of the entire REMD^{implicit} trajectory. RMSD comparison of MD trajectories (Figure 2b), on the other hand, reveals that most of the sampled conformations are quite flexible and oscillate between 1 and 9 Å throughout the length of these simulations. RMSD values obtained from MD^{Berend} were found to be slightly higher than those from MD^{Lang} in most parts of its trajectory, implying that most of the conformations (RMSD >1 Å, Figure 2b) obtained from MD trajectories are different from the starting structures. To some extent, conformations (RMSD <1 Å) close to the starting structures were also sampled at certain intervals, making their efficiency less effective in comparison to that of the REMD trajectories.

The sampling efficiency of MD and REMD simulations was monitored for different patterns of NMC attained during the progress of each trajectory. Patterns basically represent the structures classified on the basis of the type of conformational

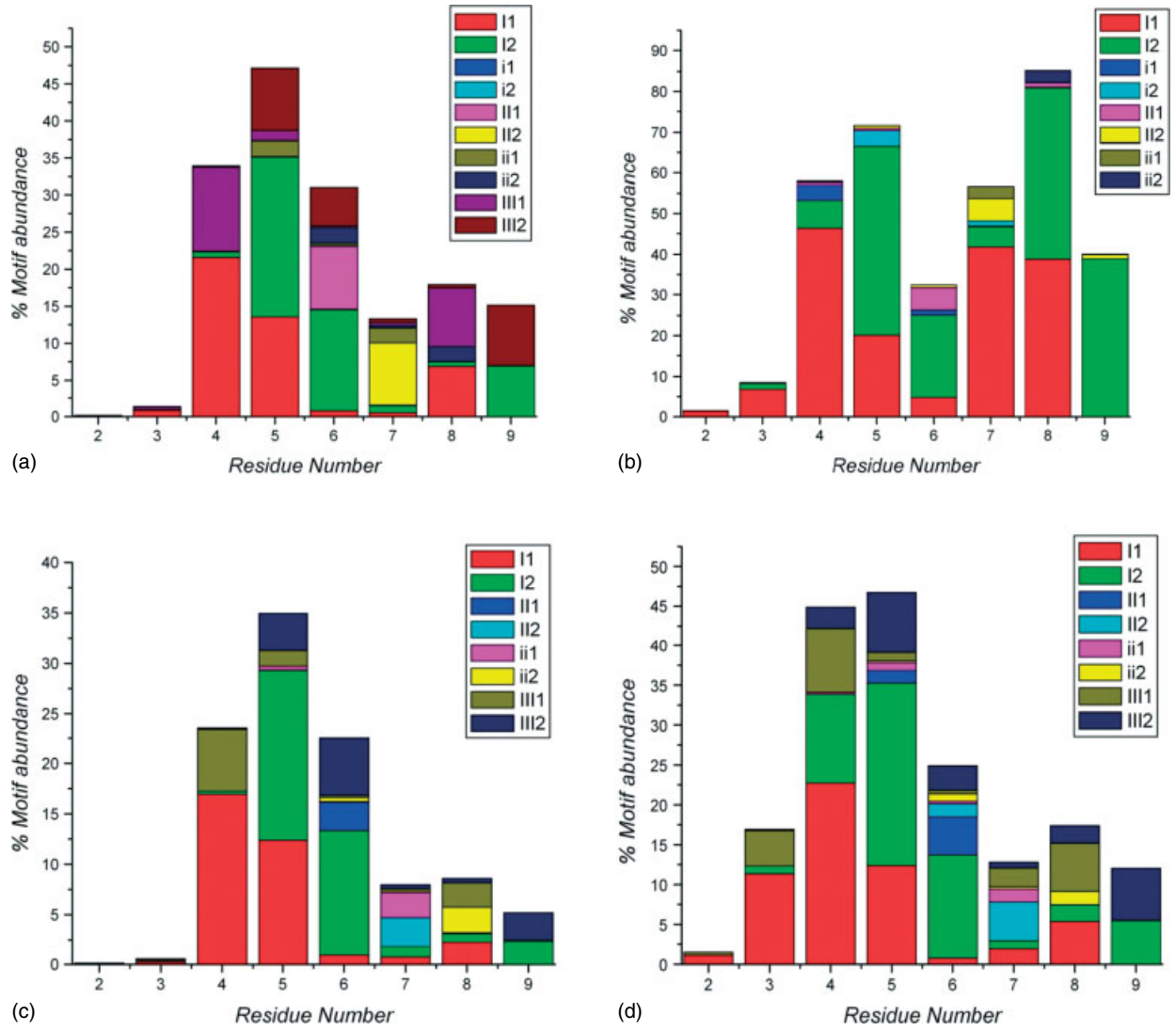

Figure 4. Conformational motif abundance attained by NMC peptide in (a) REMD^{implicit} (b) REMD^{explicit} (c) MD^{Lang} and (d) MD^{Berend} trajectories.

motifs present [30]. For this purpose, pattern profiles were computed for every snapshot in each of the trajectories using the CLASICO program; these are depicted in Figure 3. After 100 000 snapshots of REMD^{implicit} (Figure 3a) and 50 000 snapshots of REMD^{explicit} (Figure 3b) trajectories, 3206 and 1774 new patterns were obtained, respectively. Similarly, 3565 and 7981 different patterns were identified for 200 000 snapshots of MD^{Lang} (Figure 3c) and MD^{Berend} (Figure 3d) trajectories respectively. The efficiency of these trajectories in terms of generating new patterns in percentage is REMD^{explicit} (3.6%), MD^{Berend} (3.4%), REMD^{implicit} (3.2%) and MD^{Lang} (1.8%). A closer inspection of Figure 3 reveals that new patterns are generated in a regular fashion throughout the length of the REMD trajectories (Figure 3a and b), whereas in the case of MD (Figure 3c and d), peptide conformations seem to get trapped (dark areas) in regions of the conformational space at certain intervals, comparatively suggesting their restrictive nature to explore the new patterns.

The structures obtained from all the MD and REMD trajectories at 300 K were analyzed to determine the conformational motifs attained by the NMC peptide, using clasterit algorithm of the CLASICO program. The statistics of all the motifs found in the peptide for each residue are depicted in Figure 4a–d. The secondary structure motifs appear almost from the beginning of each of the trajectories. Specifically, the conformational motifs [30] obtained in REMD^{implicit} trajectory (Figure 4a) shows the predominance of β-turn type I between residues 4 and 6 with a low propensity of type III between residues 6 and 9. To some extent, β-turn type II was also observed between residues 6 and 7 in some of the conformations sampled. Figure 4b shows the profile obtained in REMD^{explicit} trajectory where the peptide predominantly exhibits β-turns type I with high propensity between residues 4 and 9 and a low propensity between residues 2 and 3. To some extent, β-turn type I (mirror conformation of β-turn type I) was also found between residues 4 and 5. In the case of MD^{Lang} (Figure 4c), the peptide adopts turns of type I between residues 4 and 9, with high propensity between residues 4 and 7 and a very low propensity between residues 7 and 9. Some conformations showing β-turn type III between residues 5 and 9 were also sampled in the MD^{Lang} trajectory. Finally, the structures exhibiting β-turn type I predominantly between residues 3 and 9 and a low propensity between residues 2–3 and 7–9 were sampled in MD^{Berend} trajectory (Figure 4d). The percentage order of β-turns

Journal of PeptideScience

Table 1. Secondary structures observed due to backbone–backbone hydrogen bond interactions and their percentages in different trajectories for NMC

Donor–acceptor	2° structure	$REMD^{explicit}$	$REMD^{implicit}$	GB^{Lang}	GB^{Berend}
2O···6N	α-helical	1.0	–	–	–
3O···7N	α-helical	4.0	10.1	10.1	1.5
5O···9N	α-helical	0.8	–	3.0	9.0
6O···10N	α-helical	3.2	–	0.4	6.0
4O···9N	π-helical	–	–	0.5	2.5
5O···10N	π-helical	0.3	6.5	1.1	4.5
10O···4N	β-turn	4.2	–	–	–
10O···4N	β-turn	5.1	–	–	–
2O···5N	β-turn	10.1	–	–	–
3O···6N	β-turn	6.5	5.1	–	–
4O···7N	β-turn	20.5	4.9	9.5	10.2
6O···9N	β-turn	7.0	–	7.2	8.7
7O···10N	β-turn	3.4	–	–	–
2O···4N	γ-turn	1.5	–	–	–
3O···5N	γ-turn	8.5	–	–	6.2
4O···6N	γ-turn	5.1	–	–	–
5O···7N	γ-turn	2.2	10.2	4.0	3.8
7O···9N	γ-turn	2.4	–	–	–
8O···10N	γ-turn	2.2	–	2.5	4.1
7O···4N	Reverse turn	–	2.5	2.3	3.2
9O···5N	Reverse turn	–	3.8	2.8	2.5
9O···7N	Reverse turn	–	3.2	1.8	1.1
8O···2N	Reverse turn	1.5	–	–	–
8O···5N	Reverse turn	–	4.2	–	–
10O···7N	Reverse turn	1.3	10.8	2.3	7.1
10O···5N	Reverse turn	1.1	2.8	–	–
10O···2N	Reverse turn	2.0	–	–	–
1O···9N	Loop	4.1	5.6	–	–
2O···9N	Loop	–	2.8	2.9	2.5
2O···10N	Loop	–	1.5	1.1	2.5
3O···10N	Loop	1.3	4.5	0.5	–
3ND1···5N	Sidechain interaction	14.0	7.8	3.4	3.5
8ND1···10N	Sidechain interaction	1.3	–	1.2	2.4

adopted by the peptide in different protocols used is $REMD^{explicit}$ (85%) > $REMD^{implicit}$ (48%) > MD^{Berend} (46%) > MD^{Lang} (35%). The percentage of helicity, on the other hand, between residues 4 and 10 in different trajectories follows the order MD^{Lang} (12.2%) > MD^{Berend} (13.1%) > $REMD^{implicit}$ (10.1%) > $REMD^{explicit}$ (3.2%). Overall these results reveal that the NMC peptide predominantly adopts β-turns type I conformations, irrespective of the method and environment used for the simulations. The current results also demonstrate that the energy barrier between folded and helical conformers is small, resulting in a population of most of the trajectories with both secondary motifs. The observed conformational behavior of NMC in the current investigations is consistent with those characterized using experimental results as reported in literature [9,10].

Hydrogen bonding is known to play an important role in determining the three-dimensional structures adopted by proteins and nucleic bases. In these macromolecules, bonding between parts of the same macromolecule causes it to fold into a specific shape, which helps determine the molecule's physiological or biochemical role. In view of the significance of H-bonding in peptides and proteins, H-bond analysis was performed on the conformational profile of NMC obtained from the different trajectories, and secondary structures were accordingly characterized. Figures 5a,b and 6a,b show the appearance of the H-bond during the progress of simulation in the $REMD^{implicit}$, $REMD^{explicit}$, MD^{Lang} and MD^{Berend} trajectories, respectively. Only those hydrogen bonds which have more than 1% existence in the trajectories have been considered for the analysis. Table 1 illustrates the type of interactions and indicates the percentage existence of the conformations in different simulations; and identifies the type of secondary structures adopted by the conformations of NMC. The first specified percentage value, regardless of where it starts from, of each trajectory in Table 1 corresponds to the first H-bond distance displayed in Figures 5a,b and 6a,b. A closer inspection of Figure 5a reveals that NMC, in $REMD^{implicit}$ trajectory, adopts some helical conformations stabilized by two hydrogen bonds between residues 3 and 7, and 5 and 9 (Table 1). However, most of the conformations in this trajectory exist preferably in the form of reverse turns (RT) and loops (Table 1). NMC conformations showing two β-turns between residues 3 and 6, and 4 and 7 were also sampled in this trajectory. $REMD^{explicit}$ (Figure 5b, Table 1) simulation sampled those conformations favorably which had a higher content of β, γ and RT in their structures as depicted by residues 2 and 10.

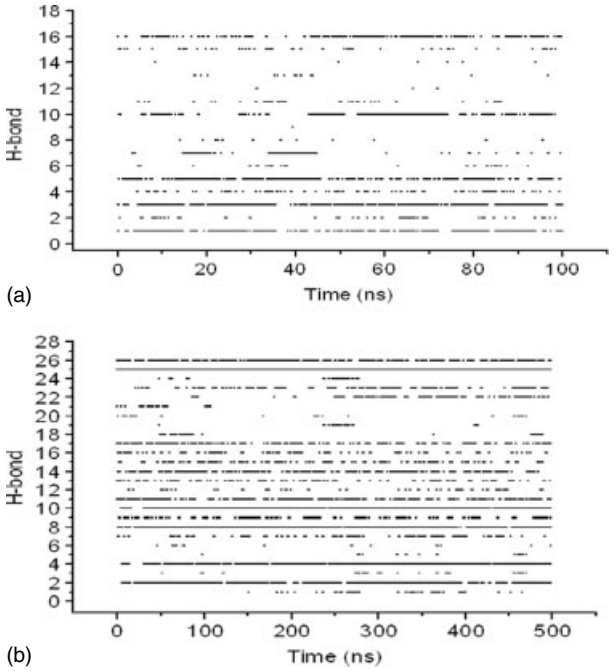

Figure 5. Progress of hydrogen bonds monitored between important residues for NMC in (a) REMD^{implicit} and (b) REMD^{explicit} trajectories. Secondary structures [α-helix, π-helix, β/γ-turns, reverse turns (RT), loop etc.] are assigned in terms of hydrogen bonding between the different residues in the peptide.

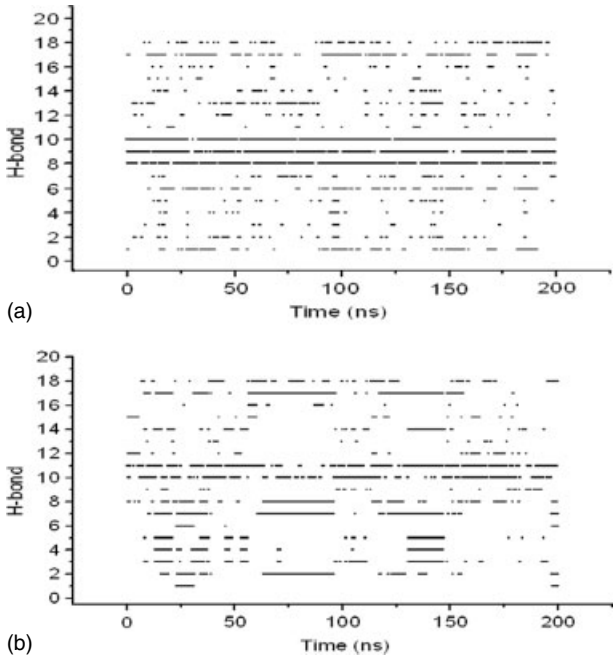

Figure 6. Progress of hydrogen bonds monitored between important residues for NMC in (a) MD^{Lang} and (b) MD^{Berend} trajectories. Secondary structures [α-helix, π-helix, β/γ-turns, reverse turns (RT), loop etc.] are assigned in terms of hydrogen bonding between the different residues in the peptide.

To some extent, conformations showing α-helical region between residues 3–7 and 6–10 were also sampled in this trajectory. The secondary structures obtained in MD^{Lang} (Figure 6a) and MD^{Berend} (Figure 6b) trajectories involves α-, π-helicals, β-, γ- and RT, and loops (Table 1) more or less in equal proportions. The helical conformations sampled in these trajectories show an α-helical region between 3–7, 5–9 and 6–10 residues (Table 1). The π-helical region was observed between residues 4–9 and 5–10 in some conformations of these trajectories (Table 1). In addition, some conformations showing sidechain–mainchain interactions between imidazolic hydrogen of residue 3 and backbone nitrogen of residue 5, observed in the rest of the simulations, were also sampled in this trajectory (Table 1). Similar kind of interactions involving the imidazolic hydrogen of residue 8 and the backbone nitrogen of residue 10 were observed in the rest of the trajectories excluding REMD^{implicit}. The number of hydrogen bonds (>1%) that appeared in the investigated protocols follows the order: REMD^{explicit} (26) > MD^{Lang} (18) = MD^{Berend} (18) > REMD^{implicit} (16), clearly suggesting the better efficiency of REMD^{explicit} to that of sample stabilized conformations.

As the computational analysis described above only provides the information regarding the average structure of the NMC peptide, a direct comparison of the performance of the different protocols used to describe the peptide folding process with the reported NMR experiments was thought to be an accurate approach. As the intensities of NMR NOEs has an inverse relation to the six power of the distance between atoms, it was thought worthwhile to perform a comparison of those with the distances measured in the computations. Owing to the nonavailability of experimental NMR distances for NMC alone, it was thought equally important to use those reported for NMC-Ni(II) complex [10] as these distances only consider residues 4–9 of NMC excluding those participating in the complexation with Ni(II). As the reported biological activity of bombesin and GRP peptides resides in their *C*-terminal residues, the utilization of NMR NOEs, which includes the middle and *C*-terminal residues of NMC (uncomplexed segment of NMC), with the present computational results was also thought to be another significant reason for this comparison. Accordingly, the clasterit algorithm of the CLASICO program was used to compute average distances, corresponding to NMR NOEs, between atoms for each of the different trajectories investigated in the present study. Only 95% of the structures of each trajectory were considered for these calculations as they were assumed to exhibit normal distribution. The results obtained from both MD and REMD trajectories were compared with NMR results by computing the overlaps between the distances obtained from NMR experiments reported in the literature and those computed from the present studies; these are depicted in Figures 7 and 8. These overlapping results involve the comparison of both long distances (i to $i+2$ type interactions) and short distances (i to $i+1$ type interactions) between the atoms. Specifically, Figure 7a reveals that the distances calculated from the REMD^{implicit} trajectory have no agreement with the NMR results, clearly suggesting the absence of NMR structures in the trajectory. REMD^{explicit} (Figure 7b), MD^{Lang} (Figure 7c) and MD^{Berend} (Figure 7d) trajectories, on the other hand, show good overlapping of the calculated distances with the NMR results, although the extent of overlap in MD structures was comparatively low. Similarly, a close inspection of the Figure 8 shows that of the 17 reported short NMR distances, there is a good agreement in 9 for those computed from the trajectory REMD^{implicit}, 16 for the trajectory REMD^{explicit}, 16 for the trajectory MD^{Lang} and 16 for trajectory MD^{Berend}, respectively. The elongation of the computed distances suggests that structures are in a dynamic equilibrium between ordered and unordered forms during the simulations.

Journal of PeptideScience

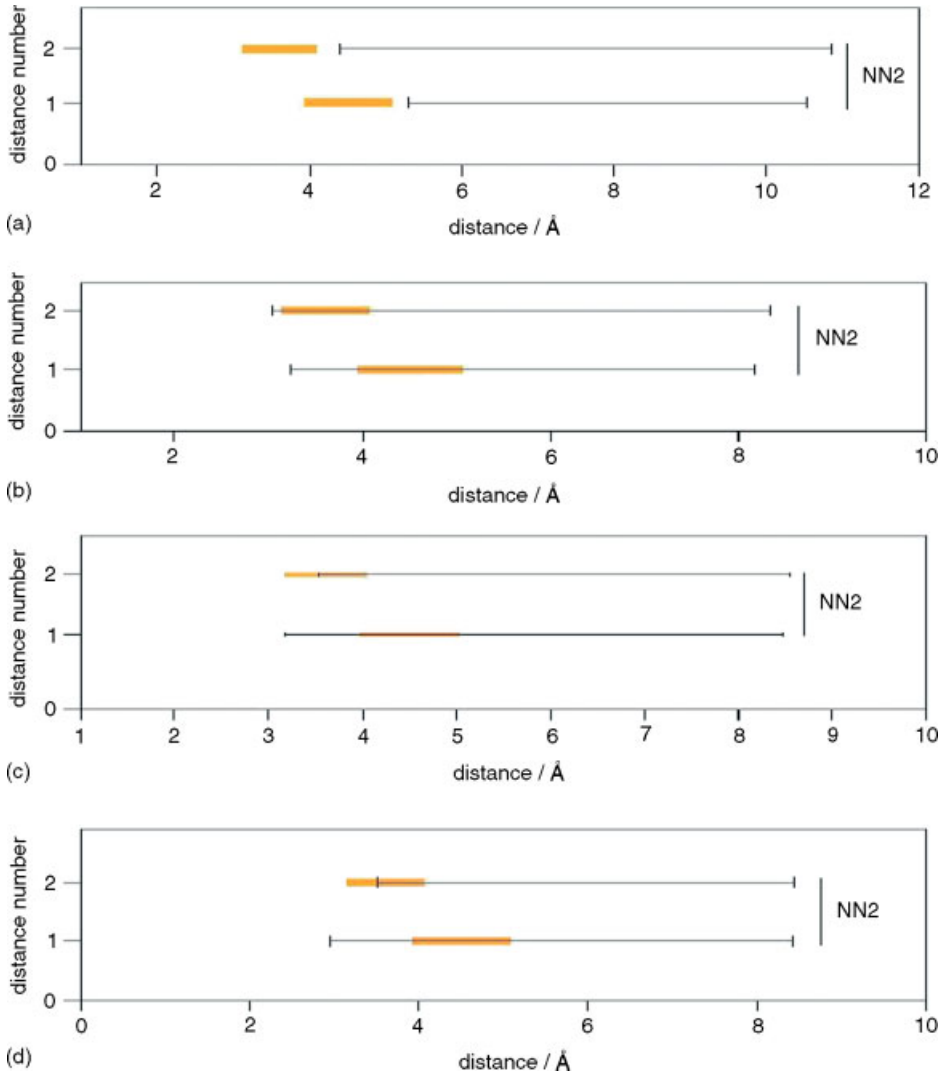

Figure 7. Comparison of NMR derived long distances (i to $i + 2$) obtained from Gasmi *et al.* [10] shown in orange and the average with the distance interval containing 95% of the structures for (a) $REMD^{implicit}$ (b) $REMD^{explicit}$ (c) MD^{Lang} and (d) MD^{Berend} trajectories.

Conclusion

Analysis of the results obtained from the $REMD^{implicit}$, MD^{Lang} and MD^{Berend} trajectories reveal that the peptide achieves folded, unfolded and helical conformations, clearly suggesting that the conformational energy difference between them is probably low and therefore accounts for the higher flexibility of NMC. $REMD^{explicit}$, on the other hand, sample preferably folded conformations with a higher content of turns (β and γ) and does not promote helicity to a considerable extent. Overall, comparison of the results obtained in the present work using different computational protocols suggests that most of the motifs of the NMC peptide adopt preferably folded conformations (turns) as compared to the helical form. Moreover, the four simulations performed produce different patterns of the configurational space sampled (Figure 3). Thus, both $REMD^{explicit}$ and $REMD^{implicit}$ simulations sample the space with new conformations appearing in a regular fashion, whereas MD trajectories (MD^{Lang} and MD^{Berend}) were observed to be get trapped in different regions of the conformational space. The sampling results obtained from different trajectories were compared with the reported experimental 2D-NMR results performed on NMC in the presence of Ni(II) metal. In particular, $REMD^{explicit}$ provides a better agreement to the long- and short-range distances. Our results suggest that REMD was better under explicit conditions than the rest of the simulations in terms of the efficiency of the exploration, and compared favorably with the experimental NMR data. Moreover, these results compliment the work of Sarkar and coworkers [10], where they have reported the role of NMC as a Cu(II) and Ni(II) transporter in the central nervous system on the basis of NMR experiments. Hence, the present work provides comprehensive information about the conformational preferences of NMC, which could assist to better understand its native conformation and point the way toward developing its new antagonists.

Acknowledgements

The authors gratefully acknowledge financial support from the Durban University of Technology, and the National Research Foundation (GUN NO 2069745). Financial support provided by the Spanish – South African Research Partnership Program through grant number 2075517 (HS2006-0022) is gratefully acknowledged.

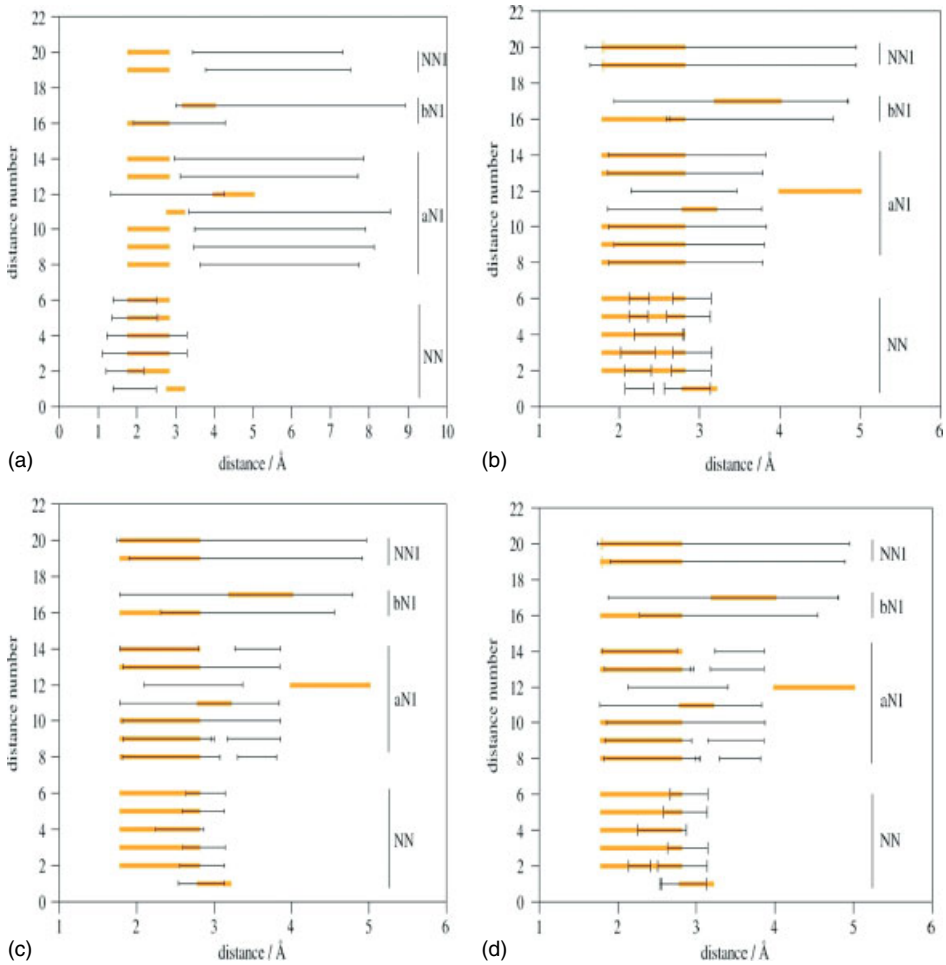

Figure 8. Comparison of NMR-derived short distances (*i* and *i* to *i* + 1) obtained from Gasmi *et al.* [10] shown in orange and the average with the distance interval containing 95% of the structures for (a) REMD^{implicit} (b) REMD^{explicit} (c) MD^{Lang} and (d) MD^{Berend} trajectories.

A PDF fellowship awarded by the NRF and DUT is gratefully acknowledged by Dr P. Singh.

References

1 Minamino N, Kangawa K, Matsuo H. Neuromedin C: a bombesin-like peptide identified in porcine spinal cord. *Biochem. Biophys. Res. Commun.* 1984; **119**: 14–20.
2 Spindel ER, Giladi E, Segerson TP, Nagalla S. Bombesin-like peptides: of ligands and receptors. *Rec. Prog. Horm. Res.* 1993; **48**: 365–391.
3 Qin Y, Ertl T, Cai R-Z, Halmos G, Schally AV. Inhibitory effect of bombesin receptor Antagonist RC-3095 on the growth of human pancreatic cancer cells *in vivo* and *in vitro*. *Cancer Res.* 1994; **54**: 1035–1041.
4 Moody TW, Carney DN, Cuttitta F, Quattrocchi K, Minna JD. I. High affinity receptors for bombesin/GRP-like peptides on human small cell lung cancer. *Life Sci.* 1985; **37**: 105–113.
5 Shin C, Mok KH, Han JH, Ahn J-H, Lim Y. Conformational analysis in solution of gastrin releasing peptide. *Biochem. Biophys. Res. Commun.* 2006; **350**: 120–124.
6 Sankararamakrishnan R. Recognition of GPCRs by peptide ligands and membrane compartments theory: structural studies of endogenous peptide hormones in membrane environment. *Biosci. Rep.* 2006; **26**: 131–158.
7 Carver JA, Collins JG, NMR identification of a partial helical conformation for bombesin in solution. *Eur. J. Biochem.* 1990; **187**: 645–650.
8 Gante J. Peptidomimetics – tailored enzyme inhibitors. *Angew. Chem., Int. Ed. Engl.* 1994; **33**: 1699–1720.
9 Polverini E, Neyroz P, Fariselli P, Casadio R, Masotti L. The effect of membranes on the conformation of Neuromedin C. *Biochem. Biophys. Res. Commun.* 1995; **214**: 663–668.
10 Gasmi G, Singer A, Forman-Kay J, Sarkar B. NMR structure of Neuromedin C, a neurotransmitter with an amino terminal Cu^{II}, Ni^{II}-binding (ATCUN) motif. *J. Peptide Res.* 1997; **49**: 500–509.
11 Arcangeli C, Bizzarri AR, Cannistraro S, Molecular dynamics simulation and essential dynamics study of mutated plastocyanin: structural, dynamical and functional effects of a disulfide bridge insertion at the protein surface. *Biophysical Chemistry* 2001; **92**: 183–199.
12 Legge FS, Budi A, Treutlein H, Yarovsky I, Protein flexibility: multiple molecular dynamics simulations of insulin chain B. *Biophysical Chemistry* 2006; **119**: 146–157.
13 Petraccone L, Garbett NC, Chaires JB, Trent JO, An integrated molecular dynamics (MD) and experimental study of higher order human telomeric quadruplexes. *Biopolymers* 2010; **93**: 533–548.
14 Stavrakoudis A, Tsoulos IG, Shenkarev ZO, Ovchinnikova TV. Molecular dynamics simulation of antimicrobial peptide arenicin-2: β-hairpin stabilization by noncovalent interactions. *Peptide Sci.* 2009; **92**: 143–155.
15 Sugita Y, Okamoto Y, Replica-exchange molecular dynamics method for protein folding. *Chem. Phys. Lett.* 1999; **314**: 141–151.
16 Pitera J, Swope W, Understanding folding and design: replica-exchange simulations of the trp-cage miniprotein. *Proc. Natl. Acad. Sci. U.S.A.* 2003; **100**: 7587–7592.
17 Gallicchio E, Zhang LY, Levy RM. Free energy surfaces of beta-hairpin and alpha-helical peptides generated by replica exchange molecular dynamics with the agbnp implicit solvent model. *Proteins* 2004; **56**: 310–321.

18 Terada T, Shimizu K. A comparison of generalized born methods in folding simulations. *Chem. Phys. Lett.* 2008; **460**: 295–299.
19 Erne D, Schwyzer R. Membrane structure of bombesin studied by infrared spectroscopy. Prediction of membrane interactions of gastrin-releasing peptide, Neuromedin B, Neuromedin C. *Biochemistry* 1987; **26**: 6316–6319.
20 Onufriev A, Bashford D, Case DA. Exploring protein native states and large-scale conformational changes with a modified generalized born model. *Proteins* 2004; **55**: 383–394.
21 Case DA, Darden TA, Cheatham TEIII, Simmerling CL, Wang J, Duke RE, Luo R, Merz KM, Wang B, Pearlman DA, Crowley M, Brozell S, Tsui V, Gohlke H, Mongan J, Hornak V, Cui G, Beroza P, Schafmeister C, Caldwell JW, Ross WS, Kollman PA. *AMBER 8*. University of California: San Francisco, 2004.
22 Weiner SJ, Kollman PA, Case DA, Singh UC, Ghio C, Alagona G, Profeta S Jr, Weiner PJ. A new force field for molecular mechanics simulation of nucleic acids and proteins. *J. Am. Chem. Soc.* 1984; **106**: 765–784.
23 Wu X, Brooks BR. Self-guided Langevin dynamics simulation method. *Chem. Phys. Lett.* 2003; **381**: 512–518.
24 Andersen HC, Molecular dynamics simulations at constant pressure and/or temperature. *J. Chem. Phys.* 1980; **72**: 2384–2393.
25 Pastor RW, Brooks BR, Szabo A. An analysis of the accuracy of Langevin and molecular dynamics algorithms. *Mol. Phys.* 1988; **65**: 1409–1414.
26 Jorgensen WL, Chandrasekhar J, Madura JD, Imprey RW, Klein ML. Comparison of simple potential functions for simulating liquid water. *J. Chem. Phys.* 1983; **79**: 926–935.
27 Darden T, York D, Pedersen L. Particle mesh Ewald: an N Log(N) method for Ewald sums in large systems. *Chem. Phys.* 1993; **98**: 10089–10092.
28 Ryckaert J-P, Ciccotti G, Berendsen HJC. Numerical integration of the cartesian equations of motion of a system with constraints: molecular dynamics of *n*-alkanes. *J. Comp. Phys.* 1977; **23**: 327–341.
29 LaFargaCPL: CLASTERIT: Project info. Available at: http://lafarga.cpl.upc.edu/projects/clusterit.
30 Corcho F, Canto J, Perez JJ. Comparative Analysis of the Conformational Profile of Substance P Using Simulated Annealing and Molecular Dynamics. *J. Comput. Chem* 2004; **25**: 1937–1952.

